

Functionalized anthradithiophenes for organic field-effect transistors†

Ming-Chou Chen,^{*a} Choongik Kim,^b Sheng-Yu Chen,^a Yen-Ju Chiang,^a Ming-Che Chung,^a Antonio Facchetti^{*b} and Tobin J. Marks^{*b}

Received 11th October 2007, Accepted 3rd January 2008

First published as an Advance Article on the web 25th January 2008

DOI: 10.1039/b715746k

Two new semiconductors for organic thin-film transistors (OTFTs), diperfluorophenyl anthradithiophene (**DFPADT**) and dimethyl anthradithiophene (**DMADT**), have been synthesized and characterized. The first material exhibits ambipolar transport in OTFT devices with field-effect mobilities (μ) of $6 \times 10^{-4} \text{ cm}^2 \text{ V}^{-1} \text{ s}^{-1}$ and $0.05 \text{ cm}^2 \text{ V}^{-1} \text{ s}^{-1}$ for electrons and holes, respectively. Therefore, diperfluorophenyl substitution was found to be effective to induce n-type transport. Dimethyl-substituted anthradithiophene (**DMADT**) was also synthesized for comparison and exhibited exclusively hole transport with carrier mobility of $\sim 0.1 \text{ cm}^2 \text{ V}^{-1} \text{ s}^{-1}$. Within this semiconductor family, OTFT carrier mobility values are strongly dependent on the semiconductor film growth conditions, substrate deposition temperatures, and gate dielectric surface treatment.

Introduction

Organic thin-film transistors (OTFTs)^{1,2} have attracted intensive attention for potential applications in flexible displays, inexpensive electronic papers, radio-frequency identification (RFID) components, and smart textiles, as well as smart memory/sensor elements in the automotive and transportation industries. Among previously developed OTFT semiconductors, most of them are hole-transporting (p-type) materials, such as pentacene derivatives,³ oligothiophenes,⁴ fused-thiophenes,⁵ and anthradithiophenes (ADTs),⁶ while n-type semiconductors are still rare.⁷ Since n-type semiconductors are crucial for the fabrication of organic p–n junctions, bipolar transistors, and complementary circuits,⁸ we are particularly interested in developing new candidates suitable for electron transport.

Anthradithiophene-based materials have demonstrated great potential for OTFT fabrication,⁶ and a solution processable p-channel ADT derivative with a hole mobility of $1.0 \text{ cm}^2 \text{ V}^{-1} \text{ s}^{-1}$ has been reported.^{6c} However, n-channel ADT semiconductors are unknown. Recently, fluoro-,^{8a} perfluoroalkyl-,^{4c,9} perfluoroaryl-,¹⁰ carbonyl-,^{8c,10a} cyano-¹¹ and trifluoromethylphenyl-^{2b,4a,5g,7c} modified oligothiophenes have been synthesized and proven to be excellent n-channel semiconductors. From single crystal X-ray diffraction (XRD) analysis, the perfluorophenyl-substituted oligothiophenes exhibit unique packing characteristics characterized by strong cofacial intermolecular packing. Enhanced electron affinity (low LUMO energy) is enabled by the strong electron-withdrawing characteristics of

the core substituents.¹⁰ Following the same design strategy, the potential use of the ADT core as a potential n-channel semiconductor candidate is proposed for the first time. The synthesis, characterization, and OTFT performance of a new diperfluorophenyl-substituted ADT compound (**DFPADT**) is presented herein. Dimethyl anthradithiophene (**DMADT**) and anthradithiophene (**ADT**) have been also synthesized and characterized for comparison.

Experimental

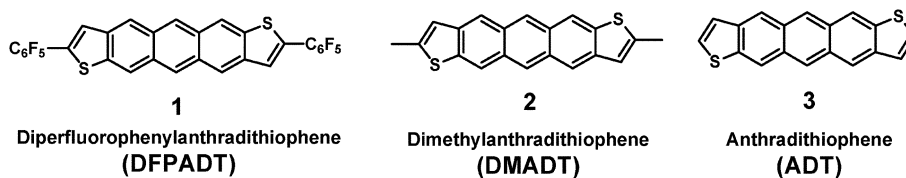
Materials and methods

All chemicals and solvents were of reagent grade obtained from Aldrich, Arco, or TCI Chemical Co. Solvents (toluene, benzene, ether, THF, and hexane) were distilled under nitrogen from Na/benzophenone ketyl, and halogenated solvents were distilled from CaH₂. Compound **3** and 2,3-bis(1,3-dioxolan-2-yl)thiophene (**6**) were prepared according to literature procedures.^{6a} ¹H and ¹³C NMR spectra were recorded on Bruker 500 or Bruker DRX-200 instruments. Chemical shifts for ¹H and ¹³C NMR spectra were referenced to solvent peaks. ¹⁹F NMR spectra were referenced to external CCl₃. DSC thermographs were carried out on a Mettler DSC 822 and calibrated with a pure indium sample with a scan rate of $10.0 \text{ }^\circ\text{C min}^{-1}$. Thermogravimetric analysis (TGA) was performed with a Perkin Elmer TGA-7 thermal analysis system using dry nitrogen as a carrier gas at a flow rate of 100 mL s^{-1} . The UV-Vis absorption and fluorescence spectra were obtained using a JASCO V-530 and a Hitachi F-4500 spectrometer, and all spectra were measured in the specified solvent at room temperature. The IR spectra were obtained using a JASCO FT/IR-4100 spectrometer. Differential pulse voltammetry experiments were performed with a CH Instruments model CHI621C Electrochemical Analyzer. All measurements were carried out at $100 \text{ }^\circ\text{C}$ with a conventional three-electrode configuration consisting of a platinum disk working electrode, an auxiliary platinum wire electrode, and a nonaqueous Ag reference electrode, and the supporting electrolyte was 0.1 M tetrabutylammonium hexafluorophosphate (TBAPF₆) in

^aDepartment of Chemistry, National Central University, Chung-Li, Taiwan, 32054, ROC. E-mail: mcchen@ncu.edu.tw; Tel: +886-3-4273253

^bDepartment of Chemistry and the Materials Research Center, Northwestern University, 2145 Sheridan Rd, Evanston, Illinois, 60208-3113, USA. E-mail: a-facchetti@northwestern.edu; t-marks@northwestern.edu; Tel: +1-847-491-3295; Tel: +1-847-491-5658

† Electronic supplementary information (ESI) available: Output characteristics of 50 nm thick **DFPADT** FET as an n-channel semiconductor; XRD patterns of 50 nm thick **DFPADT** films on HMDS-treated substrates at various temperatures. See DOI: 10.1039/b715746k



dichlorobenzene. All potentials reported are referenced to an Fc^+ /Fc internal standard. Elemental analyses were performed on a Heraeus CHN-O-Rapid elemental analyzer. Mass spectra were obtained on a JMS-700 HRMS instrument. Prime grade silicon wafers ($\text{p}^+\text{-Si}$) with ~ 300 nm ($\pm 5\%$) thermally grown oxide (from Montco Silicon) were used as device substrates.

Film deposition and characterization

All $\text{p}^+\text{-Si}/\text{SiO}_2$ substrates were cleaned by sonication in absolute ethanol (200 proof) for 3 min and then by oxygen plasma treatment for 5 min (20 W). For the SiO_2 coating layer, $-\text{SiMe}_3$ groups were introduced using hexamethyldisilazane (HMDS), deposited by placing the SiO_2 substrates in an N_2 -filled chamber saturated with HMDS vapor for 48 h. PS (5.0 mg mL^{-1} in anhydrous toluene) was spin-coated onto substrates at 5000 rpm in the air (relative humidity $\sim 30\%$) and cured in a vacuum oven at 80 °C overnight. Film thicknesses were measured by profilometry (Tencor, P10). Atomic force microscopic (AFM) images were obtained using a JEOL-5200 Scanning Probe Microscope with silicon cantilevers in the tapping mode. All of the semiconducting materials were vacuum deposited at 5×10^{-6} Torr (~ 500 Å thickness, 0.2 Å s^{-1} growth rate) at preset substrate temperatures. Thin films of organic semiconductors were analyzed by standard wide angle θ - 2θ X-ray diffraction (WAXRD) using monochromated $\text{Cu-K}\alpha$ radiation. For FET device fabrication, top-contact electrodes (~ 70 nm) were deposited by evaporating gold ($<1 \times 10^{-6}$ Torr) through a shadow mask with the channel length (L) and width (W) defined as 100 μm and 5000 μm , respectively.

OTFT and capacitance measurements

The capacitance of the bilayer dielectrics was measured on metal-insulator-semiconductor (MIS) structures using a Signatone probe station equipped with a digital capacitance meter (Model 3000, GLK Instruments). All OTFT measurements were carried out under vacuum ($<1 \times 10^{-5}$ Torr) using a Keithly 6430 subfemtoammeter and a Keithly 2400 source meter, operated by a local Labview program and GPIB communication. Mobilities (μ) were calculated in the saturation regime using the relationship:¹² $\mu_{\text{sat}} = (2I_{\text{DS}}L)/[WC_i(V_G - V_T)^2]$, where I_{DS} is the source-drain saturation current; C_i is the gate dielectric capacitance (per area), V_G is the gate voltage, and V_T is the threshold voltage. The latter can be estimated as the x intercept of the linear section of the plot of V_G vs. $(I_{\text{DS}})^{1/2}$.

Material synthesis

Synthesis of diperfluorophenylanthradithiophene (DFPADT; 1). Under nitrogen, 2.5 M $n\text{-BuLi}$ (9.6 mL in hexanes, 0.024 mol)

was slowly added into a THF solution (60 mL) of 2,3-bis(1,3-dioxolan-2-yl)thiophene (**6**; 4.56 g, 0.02 mol)^{6a} at -78 °C and the mixture was stirred for 0.5 h at this temperature. Tri-*n*-butylstannyl chloride (7.84 g, 0.026 mol) was then slowly added and the mixture was warmed to room temperature and stirred for 8 h. NH_4Cl saturated aqueous solution was added and **7** was extracted with ether, 10.1 g; yield, 97% . The product was used in the next step without further purification. ^1H NMR (CDCl_3): δ 0.90 (*t*, 9 H, CH_3), 1.28 (*m*, 6 H, CH_2), 1.48 (*t*, 6 H, CH_2), 4.02 (*m*, 4 H, $-\text{OCH}_2\text{CH}_2\text{O}-$), 4.13 (*m*, 4 H, $-\text{OCH}_2\text{CH}_2\text{O}-$), 6.06 (*s*, 1 H, *CH*), 6.35 (*s*, 1 H, *CH*), 7.14 (*s*, 1 H, *CH*). Under nitrogen, a toluene solution (60 mL) of **7** (5.18 g, 0.01 mol), bromopentafluorobenzene (1.87 mL, 0.015 mol), and tetrakis(triphenylphosphine)palladium (0.693 g, 0.6 mmol in 10 mL of toluene) was refluxed for 4 days. NH_4Cl saturated aqueous solution was added and the product was extracted with hexanes and was recrystallized to give 5-perfluorophenyl-2,3-bis(1,3-dioxolan-2-yl)thiophene, 1.95 g; yield, 50% . This product was used in the next step without further purification. ^1H NMR (CDCl_3): δ 4.04 (*m*, 4 H, $-\text{OCH}_2\text{CH}_2\text{O}-$), 4.12 (*m*, 4 H, $-\text{OCH}_2\text{CH}_2\text{O}-$), 6.06 (*s*, 1 H, *CH*), 6.40 (*s*, 1 H, *CH*), 7.50 (*s*, 1 H, *CH*). ^{19}F NMR (CDCl_3): δ -143.75 (*d*, 2F), -159.30 (*t*, 1F), -165.85 (*t*, 2F). The above dioxolanylthiophene (1.95 g) THF (10 mL) solution was added to 3 M HCl (30 mL) and stirred for 30 min at room temperature. **4a** was extracted with ether and purified by recrystallization in ether-hexanes to give yellow-brown crystals, 1.38 g; yield, 90% . ^1H NMR (CDCl_3): δ 7.99 (*s*, 1 H, *CH*), 10.38 (*s*, 1 H, *CHO*), 10.55 (*s*, 1 H, *CHO*). Anal. calcd for $\text{C}_{12}\text{H}_3\text{F}_5\text{O}_2\text{S}$: C, 47.07 ; H, 0.99 . Found: 46.92 ; H, 1.05% . Under nitrogen, a ethanol solution (60 mL) of **4a** (0.612 g, 2.0 mmol) and 1,4-cyclohexanedione (0.108 g, 1.0 mmol) was slowly added to 2.0 mL 15% KOH (in ethanol) at room temperature and the mixture was stirred overnight. The crude residue was centrifuged and washed with water (2×30 mL), methanol (2×30 mL), ether (2×30 mL) to give compound **5a** (0.63 g, 97%). The product was used in the next step without further purification. No attempt was made to separate the *syn* and the *anti* isomers.

DFPADT (1) was first prepared by reduction of the ADT quinone **5a** with LiAlH_4 . LiAlH_4 (0.152 g, 4.0 mmol) was added to an ice-cooled suspension of **5a** (0.63 g, 1.0 mmol) in dry THF (100 mL) under nitrogen atmosphere. The deep blue suspension was refluxed for 1 h. The mixture was cooled to room temperature and HCl (6 M, 40 mL) was added under cooling with ice. The mixture was then refluxed for another 3 h. The pink-red residue was centrifuged, washed with water (2×30 mL), dichloromethane (2×30 mL), MeOH (2×30 mL) and ether (2×30 mL). After drying, the crude product was again treated with LiAlH_4 and HCl and the same purified procedure was repeated to afford **1**. The product was purified by vacuum gradient

sublimation at pressures of $<10^{-4}$ Torr, giving a purple-red solid, 80 mg; yield, 12%. Because of the low yield from the above procedure, **DFPADT** (**1**) was prepared according to an alternative route.^{6a} A mixture of aluminium wire (0.208 g, 7.7 mmol) and mercuric chloride (5.2 mg, 0.02 mmol) in 30 mL of dry cyclohexanol and carbon tetrachloride (0.2 mL) was reacted overnight under mild reflux. **5a** (0.50 g, 0.77 mmol) was then added to the solution and the resulting mixture was refluxed under nitrogen for 48 h. The reaction mixture was cooled to room temperature and the solid collected by centrifugation then washed with warm cyclohexanol followed by glacial acetic acid, 10% HCl, ethanol, CHCl_3 , THF, and ether several times. The product was purified by vacuum gradient sublimation at a pressure $<10^{-4}$ Torr to give a purple-red solid, 0.16 g; yield, 34%. Mp > 400 °C (decomp.); Anal. calcd for $\text{C}_{30}\text{H}_8\text{F}_{10}\text{S}_2$: C, 57.88; H, 1.30. Found: C, 57.79; H, 1.42%.

Synthesis of dimethylantrathiodiophene (DMADT; 2). Under nitrogen, 2.5 M *n*-BuLi (6 mL in hexanes, 0.015 mol) was slowly added into a THF solution (75 mL) of 2,3-bis(1,3-dioxolan-2-yl)thiophene (**6**; 2.28 g, 0.01 mol)^{6a} at -78 °C and the mixture was stirred for 0.5 h at this temperature. Iodomethane (2.84 g, 0.02 mol) was then slowly added and the mixture was warmed to room temperature and stirred for 8 h. The product was extracted with ether ($^1\text{H NMR}$ (CDCl_3): δ 2.41 (s, 3 H, CH_3), 4.02 (m, 4 H, $-\text{OCH}_2\text{CH}_2\text{O}-$), 4.10 (m, 4 H, $-\text{OCH}_2\text{CH}_2\text{O}-$), 5.95 (s, 1 H, *CH*), 6.27 (s, 1 H, *CH*), 6.75 (s, 1 H, *CH*)), concentrated to 30 mL, 3 M HCl (20 mL) was added, and the mixture was stirred for 30 min at room temperature. Compound **4b** was extracted with ether and the crude product was then purified by recrystallization in ether–hexanes to give yellow crystals, 1.39 g; yield, 90%. $^1\text{H NMR}$ (CDCl_3): δ 2.57 (s, 3 H, CH_3), 7.29 (s, 1 H, *CH*), 10.29 (s, 1 H, *CHO*), 10.36 (s, 1 H, *CHO*). Anal. calcd for $\text{C}_7\text{H}_6\text{O}_2\text{S}$: C, 54.53; H, 3.92. Found: 54.25; H, 4.11%. Under nitrogen, a ethanol solution (60 mL) of **4b** (0.788 g, 5.0 mmol) and 1,4-cyclohexanedione (0.275 g, 2.5 mmol) was slowly added to 2.5 mL 15% KOH (in ethanol) at room temperature and the mixture was stirred for 1 h. The crude solid product was collect

by centrifugation and washed with water (2×30 mL), methanol (2×30 mL), ether (2×30 mL) to give compound **5b** (0.86 g, 97%). $^1\text{H NMR}$ (CDCl_3): δ 2.68 (s, 6 H, CH_3), 7.26 (s, 2 H), 8.62 (s, 2 H), 8.76 (s, 2 H). The product was used in the next step without further purification. No attempt was made to separate the *syn* and the *anti* isomers.

DMADT (2) was prepared by reduction of the ADT quinone **5b** with LiAlH_4 . LiAlH_4 (0.152 g, 4.0 mmol) was added to an ice-cooled suspension of **5b** (0.348 g, 1.0 mmol) in dry THF (100 mL) under nitrogen atmosphere. Through a similar procedure as mentioned above, **2** was obtained as a bright orange solid (0.19 g) in 60% yield. Mp > 400 °C (decomp.); Anal. calcd for $\text{C}_{20}\text{H}_{14}\text{S}_2$: C, 75.43; H, 4.43. Found: C, 75.22; H, 4.50%. MS (EI) *m/z* calcd for $\text{C}_{20}\text{H}_{14}\text{S}_2$: 318 (M^+).

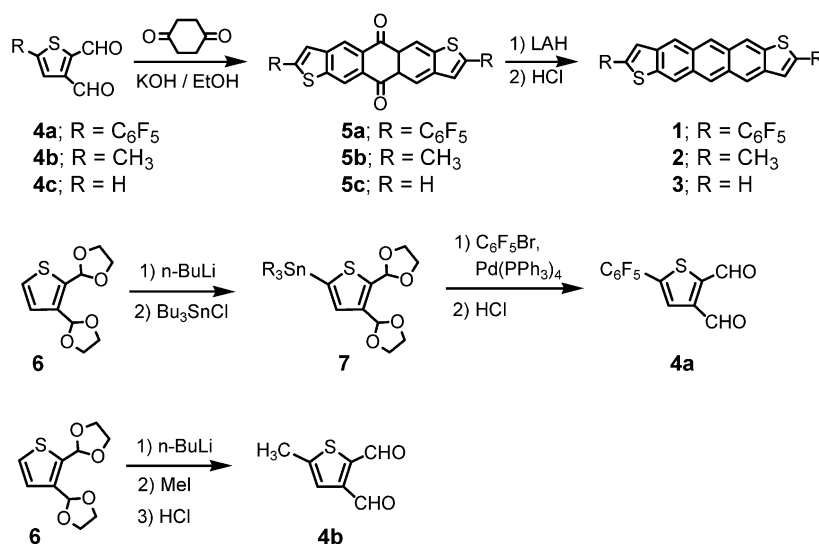
Results and discussion

Synthesis

The synthesis of functionalized anthradithiophenes **1** and **2** was achieved according to Scheme 1 following known ADT core synthetic approaches.⁶ Starting from 5-perfluorophenyl-2,3-thiophenedicarboxaldehyde (**4a**), **DFPADT** (**1**) was obtained in $\sim 30\%$ yield, while **DMADT** (**2**) was obtained in $\sim 60\%$ yield from **4b**. **4a** was prepared in $\sim 45\%$ yield by Stille coupling reaction of 5-(tributylstannyl)-2,3-bis(1,3-dioxolan-2-yl)-thiophene (**7**) with bromopentafluorobenzene. The dimethyl derivative **4b** was obtained in $\sim 90\%$ yield from the methylation of 2,3-bis(1,3-dioxolan-2-yl)thiophene **6**. **ADT** (**3**) was synthesized according to a known procedure.⁶ For both ADT derivatives **1** and **2**, differential scanning calorimetry (DSC) measurements did not show any melting endotherm up to 400 °C. Thermogravimetric analysis plots demonstrate weight loss only after heating above 400 °C.

UV-Vis spectroscopy

As shown in Fig. 1A, the UV-Vis absorption spectrum of **DFPADT** (**1**) in CHCl_3 is significantly red shifted ($\lambda_{\text{max}} = 515$



Scheme 1 Synthesis of compounds 1–3.

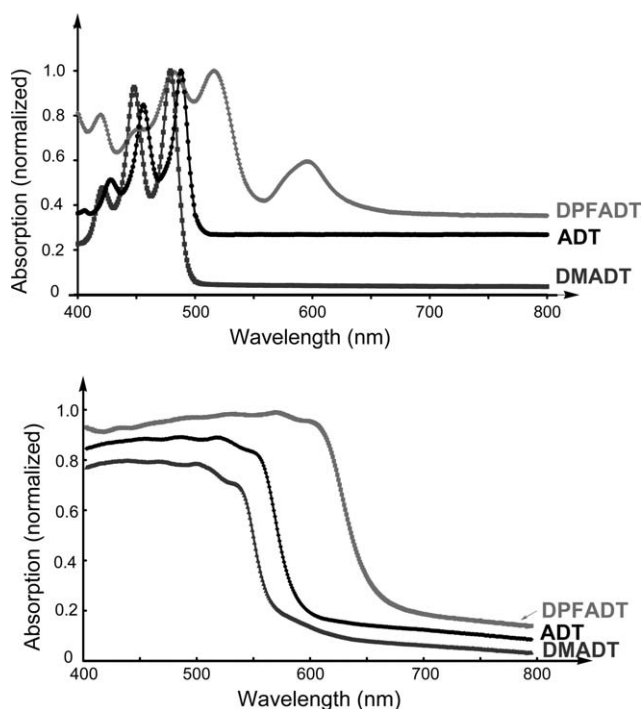


Fig. 1 (A) UV-Vis spectra of ADTs 1–3 in CHCl_3 , (B) Reflection UV-Vis spectra of ADTs (1–3) powder.

nm) compared to ADT (3) ($\lambda_{\text{max}} = 488$ nm) and DMADT (2) ($\lambda_{\text{max}} = 479$ nm). This result is in line with the substituent group directing effects.¹⁰ Furthermore, DFPADT spectrum exhibits an additional absorption located at $\lambda_{\text{max}} = 595$ nm, indicating considerable π -electron delocalization extending from the ADT core to the two electron withdrawing perfluorophenyl substituents. The HOMO–LUMO energy gaps calculated from the onset of the absorption are 2.50 eV for DMADT, 2.46 eV for ADT, and 1.95 eV for DFPADT. The absorption red shifts going from 3 and 2 to 1 were also observed in reflection UV-Vis absorption spectra of 1–3 powders (Fig. 1B). This result suggests large core conjugation for 1 in the solid state and/or possible formation of J-aggregates.^{2b,n}

The photooxidative stability of the ADT derivatives was investigated by monitoring the absorbance decay at λ_{max} of 1–3 in aerated CHCl_3 solutions exposed to white light (fluorescent lamp) at room temperature. Under these conditions for 24 h, DFPADT exhibits the longest life time ($\sim 37\%$ decay), demonstrating the substituent effects on molecular stability, while DMADT shows the shortest ($\sim 75\%$ decay). ADT exhibits $\sim 45\%$ decay under the same conditions. Clearly, perfluorophenyl substitution stabilizes the ADT core as previously observed for thiophene- and pentacene-based derivatives.¹³

Differential pulse voltammetry

Differential pulse voltammograms (DPV) of 1–3 were recorded in dichlorobenzene at 100 °C and the DPV plots are shown in Fig. 2.¹⁴ The differential pulse voltammogram of DFPADT exhibits an oxidation peak at +1.04 V and a reduction peak at -0.94 V (ferrocene/ferrocenium as internal standard). Both the oxidation and reduction potentials of ADT ($E_{\text{ox}} = +0.94$ V,

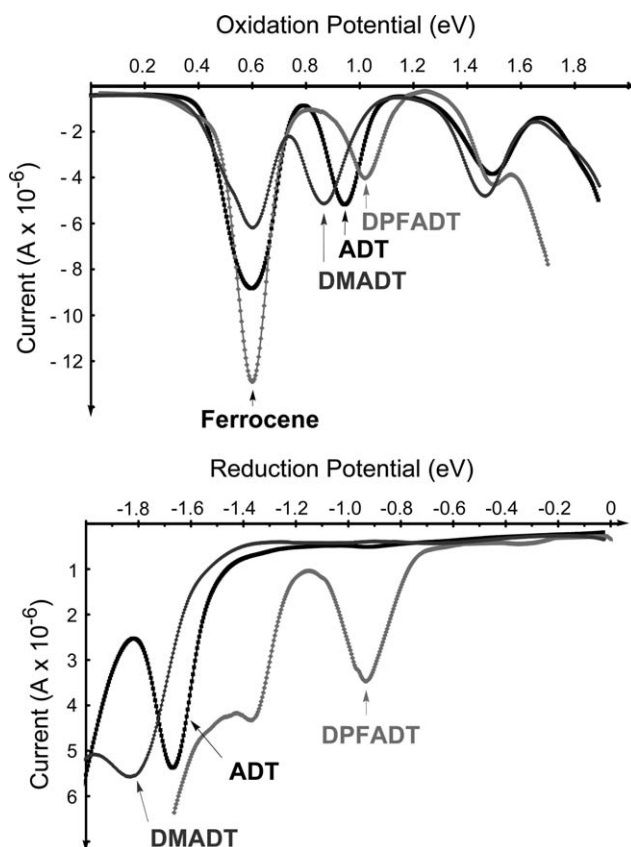


Fig. 2 DPV of compounds 1–3 in dichlorobenzene. (A) Oxidation and (B) reduction scans.



Fig. 3 The electrochemically derived HOMO and LUMO energies of compounds 1–3.

$E_{\text{red}} = -1.67$) and DMADT ($E_{\text{ox}} = +0.86$ V, $E_{\text{red}} = -1.83$) are shifted to more positive values than those observed for DFPADT (Fig. 2), which can be attributed to the electron-withdrawing effect of the perfluorophenyl substituents. The derived molecular orbital energy orderings (Fig. 3) demonstrate that fluoroaryl substitution strongly lowers both HOMO and LUMO energies.^{8c,10b} The electrochemically derived HOMO–LUMO energy gaps are 1.98 eV for DFPADT, 2.61 eV for ADT, and 2.69 eV for DMADT. The calculated energy levels from DPV plots are consistent with those obtained from UV-Vis spectroscopy.

Field-effect transistor performance

Top-contact OTFTs were fabricated by vapor-depositing 50 nm thick 1–3 films on bare, hexamethyldisilazane (HMDS)-treated, or polystyrene (PS)-coated $\text{p}^+\text{-Si/SiO}_2$ substrates, followed by Au deposition through a shadow mask to define the source

and drain electrodes. The substrate temperature (T_D) during semiconductor film deposition was controlled with a thermocouple. OTFT characterization was performed under vacuum and the device performance data are summarized in Table 1.¹⁵ For data analysis it is clear that ADT derivative-based OTFT performance strongly depends on both dielectric surface treatment and T_D value. As a general trend, for all compounds, p-channel performance increases at higher T_D s, similarly to the previous ADT derivatives.⁶ As T_D increases, the hole mobilities and $I_{on} : I_{off}$ increase, while the threshold voltage shifts to less negative values. Overall, **DMADT**-based OTFTs perform better on HMDS-treated substrates,¹⁶ whereas those based on **DFPADT** exhibit the best performance on PS-coated p⁺-Si/SiO₂ substrates. **DFPADT**-based TFTs exhibit electron mobilities $\sim 100\times$ lower than the hole mobilities. This result is typical for most fluorinated semiconductors¹⁷ where electron transport is much more sensitive than hole transport.

For **DFPADT**-based TFTs, the highest hole mobility (μ_h) of $0.05 \text{ cm}^2 \text{ V}^{-1} \text{ s}^{-1}$ is observed on PS-coated substrates ($T_D = 150^\circ \text{C}$) with a threshold voltage (V_T) of -25 V and $I_{on} : I_{off}$ of $\sim 10^6$ (Fig. 4a), while the highest electron mobility (μ_e) of $\sim 6 \times 10^{-4} \text{ cm}^2 \text{ V}^{-1} \text{ s}^{-1}$ is observed on the same substrates ($T_D = 25^\circ \text{C}$) with a threshold voltage (V_T) of $+55 \text{ V}$ and $I_{on} : I_{off}$ of $\sim 10^2$ (Fig. 4b). A distinctive feature of ambipolar transport can be observed in the output characteristic of **DFPADT** (Fig. S1 in ESI[†]) where for $V_G \ll V_{DS}$ the I_{DS} increases considerably with increasing V_{DS} .¹⁸ To our knowledge this is the first

Table 1 Charge carrier mobilities ($\mu/\text{cm}^2 \text{ V}^{-1} \text{ s}^{-1}$)^a, current on/off ratios ($I_{on} : I_{off}$), and threshold voltages (V_T/V) for OFETs fabricated with semiconductors **1** to **3**

Compound	Substrate	T_D ^b /°C	μ	$I_{on} : I_{off}$	V_T	
DFPADT (1) (p-type)	Bare	25	5.0×10^{-6}	10^3	-35	
			HMDS	7.0×10^{-6}	10^3	-34
			PS	7.3×10^{-6}	10^3	-29
	Bare	85	6.8×10^{-6}	10^3	-31	
			HMDS	1.7×10^{-5}	10^3	-34
			PS	1.3×10^{-5}	10^3	-35
	Bare	120	1.6×10^{-4}	10^2	-21	
			HMDS	5.0×10^{-4}	10^3	-29
			PS	3.8×10^{-4}	10^4	-39
Bare	150	3.0×10^{-3}	10^5	-31		
		HMDS	4.0×10^{-2}	10^6	-27	
		PS	4.8×10^{-2}	10^6	-25	
DFPADT (1) (n-type)	HMDS	25	2.6×10^{-6}	10^1	+142	
			PS	6.1×10^{-4}	10^2	+55
			HMDS	6.0×10^{-7}	10^1	+145
	PS	85	2.0×10^{-5}	10^3	+82	
			HMDS	1.9×10^{-4}	10^1	+109
			PS	2.2×10^{-5}	10^3	+130
	HMDS	150	2.0×10^{-4}	10^1	+106	
			PS	3.0×10^{-4}	10^3	+58
			DMADT (2) (p-type)	Bare	25	0.048
HMDS	0.062	10^4				-19
PS	0.070	10^4				-33
Bare	85	0.070	10^2	-3		
		HMDS	0.10	10^3	-8	
		PS	0.011	10^5	-10	
ADT (3) (p-type)	Bare	25	0.008	10^5	-20	
			HMDS	0.010	10^5	-21
			PS	0.012	10^5	-33

^a Calculated in the saturation regime. Typical standard deviations are <10%. ^b Substrate deposition temperature.

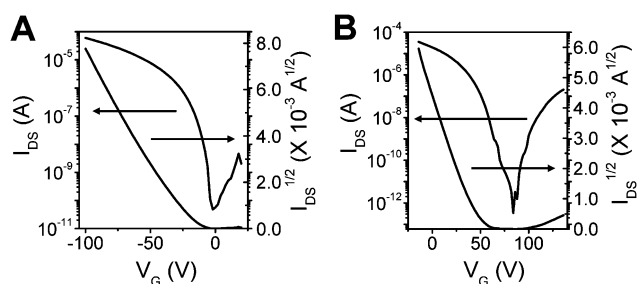


Fig. 4 Transfer plots of OTFT devices fabricated with **DFPADT**. A. p-type character; film deposited at $T_D = 150^\circ \text{C}$. B. n-type character; film deposited at $T_D = 25^\circ \text{C}$.

report of an ambipolar ADT derivative. Clearly, ADT end-substitution with strongly electron withdrawing perfluorophenyl groups does promote electron transport as previously demonstrated in other studies,¹⁰ but it does not prevent efficient hole transport.

Fluoroarene-free **DMADT (2)** only exhibits hole transport with the highest mobilities (μ_h) of $\sim 0.1 \text{ cm}^2 \text{ V}^{-1} \text{ s}^{-1}$ on HMDS-treated substrates ($T_D = 85^\circ \text{C}$), a threshold voltage (V_T) of -8 V , and $I_{on} : I_{off}$ of $\sim 10^3$ (Fig. 5), which is comparable to the TFT performance of previously reported dihexyl-substituted ADT ($\sim 0.15 \text{ cm}^2 \text{ V}^{-1} \text{ s}^{-1}$ at 85°C).⁶ ADT (**3**) is also a p-type semiconductor and exhibits maximum hole mobilities (μ_h) of $0.01 \text{ cm}^2 \text{ V}^{-1} \text{ s}^{-1}$, a threshold voltage (V_T) of -21 V , and $I_{on} : I_{off}$ of $\sim 10^5$ on HMDS-treated substrates ($T_D = 25^\circ \text{C}$), which is similar to the literature values.¹⁹

The present ADT-based compounds also possess great oxidative stability, as previously demonstrated for other end-substituted anthradithiophenes.⁶ Note that pentacene suffers from oxidative instability,²⁰ making the ADT family attractive for future application. OTFTs fabricated with **1** and **2** exhibited excellent stability when the devices were kept in the dark under ambient conditions for several months. Negligible degradation of p-channel mobility, threshold voltage, and I_{on}/I_{off} over six months were observed for **DFPADT**-based TFTs, demonstrating the advantages of using this stable ADT core for next-generation solution processable semiconductors.²¹ One drawback of n-type TFTs based on **DFPADT** is the very large threshold voltages. This may be related to the quite negative reduction potential (much more negative than typical n-type semiconductors) of **DFPADT** and/or the high injection barrier between the LUMO of **DFPADT** (3.26 eV) and the gold electrode work function (5.1 eV).

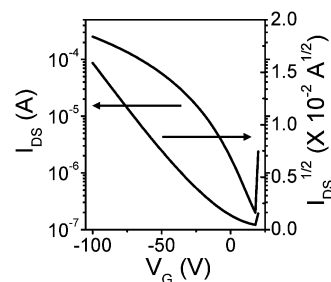


Fig. 5 Transfer plot of OTFT device fabricated with **DMADT**, film deposited at $T_D = 85^\circ \text{C}$.

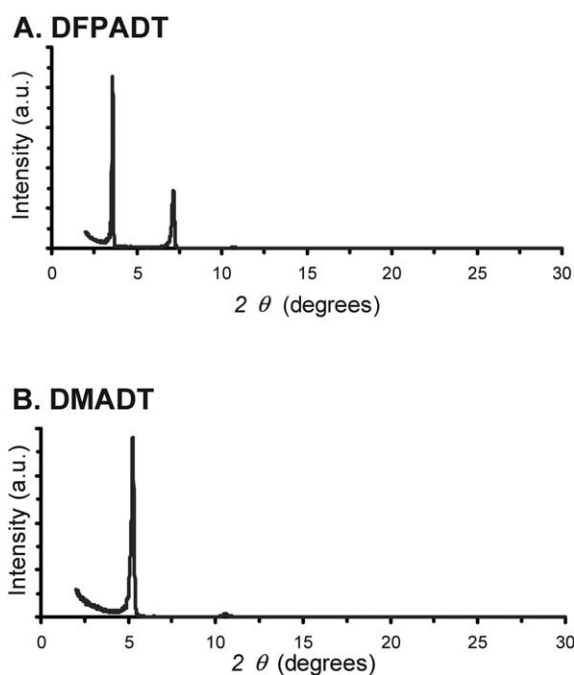


Fig. 6 XRD patterns of 50 nm thick films of the indicated semiconductors grown on HMDS-treated substrates at $T_D = 85^\circ\text{C}$.

To investigate ADT-based semiconductor film microstructure and correlate it to the corresponding TFT performance, wide-angle X-ray diffraction (WAXRD) experiments were performed for the **DFPADT** (**1**) and **DMADT** (**2**) films. Fig. 6 shows XRD patterns of **1** and **2** films deposited at $T_D = 85^\circ\text{C}$ on HMDS-treated substrates, demonstrating that these films are highly crystalline. For both films only one set of strong reflections is observed in the θ - 2θ scan, with the first reflection located at $2\theta = 3.75^\circ$ for **1** and $2\theta = 5.25^\circ$ for **2**. These angles correspond to a film d -spacing of 24.6 \AA for **1** and 16.8 \AA for **2** and demonstrate an end-on-substrate molecular orientation.²² Since the TFT performance of **1** is quite sensitive to the substrate temperature, the XRD patterns were also examined at various T_D s (ESI† Fig. S2). As the T_D increases, the first Bragg reflection intensity increases and shifts to smaller angle corresponding to a slightly larger d -spacing. This result may partially account for the improved TFT performance. However, film morphology variations with T_D may also play an important role. Indeed, AFM images of the ADT films demonstrate that film growth depends significantly on both T_D and the dielectric surface treatment.⁹ In all cases, semiconductor films deposited at 25°C consist of small grains (Fig. 7A, C and 8A), likely resulting from slow molecular diffusion on the cold dielectric surface of the film nucleation sites.²³ For the films of **DFPADT**, as T_D is increased from 25°C to 150°C , the film grains become larger and longer (Fig. 7B, D and 8B) on either surface treatment. This result corroborates the improved electron mobilities of **DFPADT**-based TFTs when the films are deposited at higher substrate temperatures (see Table 1). In the case of **DMADT**, the grain size of the films grown on HMDS-treated substrates at 85°C (Fig. 8B) is extremely large (*ca.* $1\text{ }\mu\text{m}$) in agreement with the higher device performance.

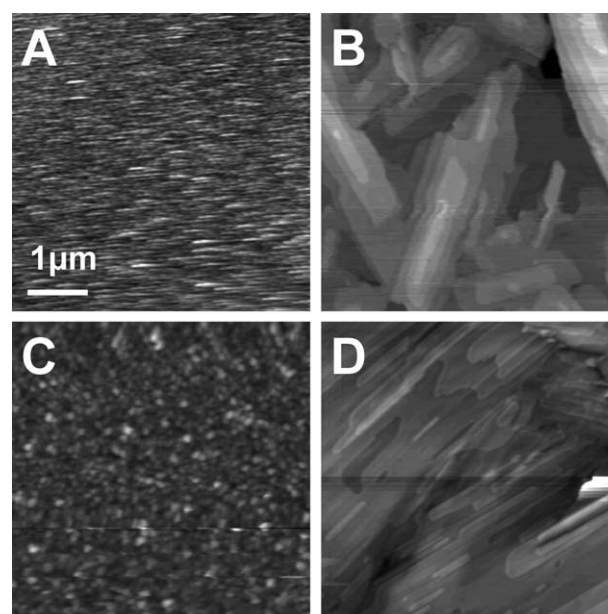


Fig. 7 AFM images ($5\text{ }\mu\text{m} \times 5\text{ }\mu\text{m}$) of 50 nm thick films of **DFPADT** grown on HMDS-treated substrates at A $T_D = 25^\circ\text{C}$, B $T_D = 150^\circ\text{C}$. **DFPADT** grown on PS-coated substrates at C $T_D = 25^\circ\text{C}$, D $T_D = 150^\circ\text{C}$.

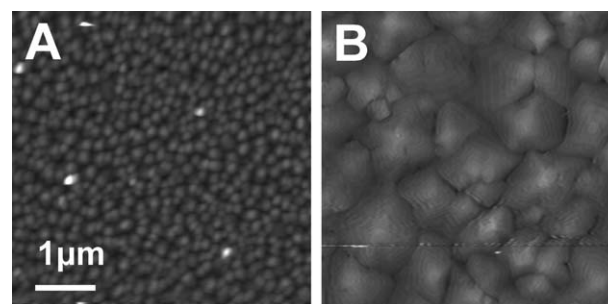


Fig. 8 AFM images ($5\text{ }\mu\text{m} \times 5\text{ }\mu\text{m}$) of 50 nm thick films of **DMADT** grown on HMDS-treated Si/SiO_2 substrates. A at $T_D = 25^\circ\text{C}$, B at $T_D = 85^\circ\text{C}$.

Conclusions

In summary, the first diperfluorophenyl-substituted anthradithiophene (**DFPADT**) has been synthesized and exhibited TFT ambipolar transport. The perfluorophenyl group was found to be effective in inducing n-channel transport while preserving p-channel transport. The devices based on **DFPADT** exhibit field-effect mobilities (μ) of $6 \times 10^{-4}\text{ cm}^2\text{ V}^{-1}\text{ s}^{-1}$ for electrons and $0.05\text{ cm}^2\text{ V}^{-1}\text{ s}^{-1}$ for holes. Dimethyl anthradithiophene (**DMADT**) was also synthesized for comparison and exhibited only p-channel transport with hole mobilities approaching $0.1\text{ cm}^2\text{ V}^{-1}\text{ s}^{-1}$. The carrier mobilities of these derivatives depend on the substrate deposition temperature and dielectric surface treatment. P-Type operation of these ADT-based OTFTs exhibited excellent stability over months (nearly one year), demonstrating the advantages of using this core for the realization of solution processable organic semiconductors.

Acknowledgements

We thank the NSF-MRSEC program through the Northwestern Materials Research Center (DMR-0520513) and Polyera Corporation for financial support. Financial assistance for this research was partially provided by the National Science Council, Republic of China (Grant Number NSC 95-2113-M-008-008-MY2).

References and notes

- For recent reviews on this topic, see: (a) J. E. Anthony, *Chem. Rev.*, 2006, **106**, 5028; (b) M. Chabinyk and Y.-L. Loo, *J. Macromol. Sci., Polym. Rev.*, 2006, **46**, 1; (c) A. Dodabalapur, *Nature*, 2005, **434**, 151; (d) H. Sirringhaus, *Adv. Mater.*, 2005, **17**, 2411; (e) A. Facchetti, M.-H. Yoon and T. J. Marks, *Adv. Mater.*, 2005, **17**, 1705; (f) C. R. Newman, C. D. Frisbie, D. A. da Silva Filho, J.-L. Bredas, P. C. Ewbank and K. R. Mann, *Chem. Mater.*, 2004, **16**, 4436; (g) G. Horowitz, *J. Mater. Res.*, 2004, **19**, 1946; (h) C. D. Dimitrakopoulos and P. R. L. Malenfant, *Adv. Mater.*, 2002, **14**, 99.
- For recent studies, see: (a) Y. Sun, L. Tan, S. Jiang, H. Qian, Z. Wang, D. Yan, C. Di, Y. Wang, W. Wu, G. Yu, S. Yan, C. Wang, W. Hu, Y. Liu and D. Zhu, *J. Am. Chem. Soc.*, 2007, **129**, 1882; (b) T. Kono, D. Kumaki, J.-I. Nishida, T. Sakanoue, M. Kakita, H. Tada, S. Tokito and Y. Yamashita, *Chem. Mater.*, 2007, **19**, 1218; (c) H. Z. Chen, M. M. Ling, X. Mo, M. M. Shi, M. Wang and Z. Bao, *Chem. Mater.*, 2007, **19**, 816; (d) X. Gao, W. Wu, Y. Liu, S. Jiao, W. Qiu, G. Yu, L. Wang and D. Zhu, *J. Mater. Chem.*, 2007, **17**, 736; (e) O. D. Jurchescu, M. Popinciuc, B. J. van Wees and T. T. M. Palstra, *Adv. Mater.*, 2007, **19**, 688; (f) T. Okamoto, K. Kudoh, A. Wakamiya and S. Yamaguchi, *Chem.-Eur. J.*, 2007, **13**, 548; (g) X. Cai, C. P. Gerlach and C. D. Frisbie, *J. Phys. Chem. C*, 2007, **111**, 452; (h) Y. Li, Y. Wu, P. Liu, Z. Prostran, S. Gardner and B. S. Ong, *Chem. Mater.*, 2007, **19**, 418; (i) S. E. Koh, B. Delley, J. E. Medvedeva, A. Facchetti, A. J. Freeman, T. J. Marks and M. A. Ratner, *J. Phys. Chem. B*, 2006, **110**, 24361; (j) Y. Sun, Y. Liu, Y. Ma, C. Di, Y. Wang, W. Wu, G. Yu, W. Hu and D. Zhu, *Appl. Phys. Lett.*, 2006, **88**, 242113; (k) H. Wang, J. Wang, X. Yan, J. Shi, H. Tian, Y. Geng and D. Yan, *Appl. Phys. Lett.*, 2006, **88**, 133508; (l) Naraso, J.-i. Nishida, D. Kumaki, S. Tokito and Y. Yamashita, *J. Am. Chem. Soc.*, 2006, **128**, 9598; (m) H. Meng, F. Sun, M. B. Goldfinger, F. Gao, D. J. Londono, W. J. Marshal, G. S. Blackman, K. D. Dobbs and D. E. Keys, *J. Am. Chem. Soc.*, 2006, **128**, 9304; (n) M.-H. Yoon, A. Facchetti, C. E. Stern and T. J. Marks, *J. Am. Chem. Soc.*, 2006, **128**, 5792; (o) A. Zen, A. Bilge, F. Galbrecht, R. Alle, K. Meerholz, J. Grenzer, D. Neher, U. Scherf and T. Farrell, *J. Am. Chem. Soc.*, 2006, **128**, 3914; (p) T. D. Anthopoulos, S. Setayesh, E. S. Mts. de Colle, E. Cantatore, B. de Boer, P. W. M. Blom and D. M. de Leeuw, *Adv. Mater.*, 2006, **18**, 1900; (q) G. S. Tulevski, Q. Miao, A. Afzali, T. O. Graham, C. R. Kagan and C. Nuckolls, *J. Am. Chem. Soc.*, 2006, **128**, 1788; (r) R. Schmidt, S. Götting, D. Leusser, D. Stalke, A. Krause and F. Würthner, *J. Mater. Chem.*, 2006, **16**, 3708; (s) B. Wex, B. R. Kaafarani, R. Schroeder, L. A. Majewski, P. Burckel, M. Grell and D. C. Neckers, *J. Mater. Chem.*, 2006, **16**, 1121.
- (a) M. M. Payne, S. R. Parkin and J. E. Anthony, *J. Am. Chem. Soc.*, 2005, **127**, 8028; (b) C. R. Swartz, S. R. Parkin, J. E. Bullock, J. E. Anthony, A. C. Mayer and G. G. Malliaras, *Org. Lett.*, 2005, **7**, 3163; (c) D. J. Gundlach, Y. Y. Lin, T. N. Jackson and S. F. Nelson, *Appl. Phys. Lett.*, 2002, **80**, 2925; (d) H. Meng, M. Bendikov, G. Mitchell, R. Helgeson, F. Wudl, Z. Bao, T. Siegrist, C. Kloc and C. H. Chen, *Adv. Mater.*, 2003, **15**, 1090; (e) Y. Li, Y. Wu, P. Liu, Z. Prostran, S. Gardner and B. S. Ong, *Chem. Mater.*, 2007, **19**, 418.
- (a) H. K. Tian, J. W. Shi, D. H. Yan, L. X. Wang, Y. H. Geng and F. S. Wang, *Adv. Mater.*, 2006, **18**, 2149; (b) S. Ando, R. Murakami, J. Nishida, H. Tada, Y. Inoue, S. Tokito and Y. Yamashita, *J. Am. Chem. Soc.*, 2005, **127**, 14996; (c) A. Facchetti, J. Letizia, M.-H. Yoon, M. Mushrush, H. E. Katz and T. J. Marks, *Chem. Mater.*, 2004, **16**, 4715; (d) M. Halik, H. Klauk, U. Zschieschang, G. Schmid, S. Ponomarenko, S. Kirchmeyer and W. Weber, *Adv. Mater.*, 2003, **15**, 917.
- (a) D. Kumaki, S. Ando, S. Shimono, Y. Yamashita, T. Umeda and S. Tokito, *Appl. Phys. Lett.*, 2007, **90**, 053506; (b) X. Cai, C. P. Gerlach and C. D. Frisbie, *J. Phys. Chem. C*, 2007, **111**, 452; (c) K. Takimiya, Y. Kunugi, Y. Konda, H. Ebata, Y. Toyoshima and T. Otsubo, *J. Am. Chem. Soc.*, 2006, **128**, 3044; (d) Y. M. Sun, Y. Q. Ma, Y. Q. Liu, Y. Y. Lin, Z. Y. Wang, Y. Wang, C. A. Di, K. Xiao, X. M. Chen, W. F. Qiu, B. Zhang, G. Yu, W. P. Hu and D. Zhu, *Adv. Funct. Mater.*, 2006, **16**, 426; (e) K. Xiao, Y. Liu, T. Qi, W. Zhang, F. Wang, J. Gao, W. Qiu, Y. Ma, G. Cui, S. Chen, X. Zhan, G. Yu, J. Qin, W. Hu and D. Zhu, *J. Am. Chem. Soc.*, 2005, **127**, 13281; (f) X. Zhang, A. P. Cote and A. J. Matzger, *J. Am. Chem. Soc.*, 2005, **127**, 10502; (g) S. Ando, J. Nishida, H. Tada, Y. Inoue, S. Tokito and Y. Yamashita, *J. Am. Chem. Soc.*, 2005, **127**, 5336; (h) T. Ozturk, E. Ertaş and O. Mert, *Tetrahedron*, 2005, **61**, 11055; (i) P. Leriche, J.-M. Raimundo, M. Turbiez, V. Monroche, M. Allain, F.-X. Sauvage, J. Roncali, P. Frere and P. J. Skabara, *J. Mater. Chem.*, 2003, **13**, 1324.
- (a) J. G. Laquindanum, H. E. Katz and A. J. Lovinger, *J. Am. Chem. Soc.*, 1998, **120**, 664; (b) M. M. Payne, S. A. Odom, S. R. Parkin and J. E. Anthony, *Org. Lett.*, 2004, **6**, 3325; (c) M. M. Payne, S. R. Parkin, J. E. Anthony, C.-C. Kuo and T. N. Jackson, *J. Am. Chem. Soc.*, 2005, **127**, 4986.
- For recent n-type OTFT studies, see: (a) B. A. Jones, A. Facchetti, M. R. Wasielewski and T. J. Marks, *J. Am. Chem. Soc.*, 2007, **129**, 15259; (b) Z. Wang, C. Kim, A. Facchetti and T. J. Marks, *J. Am. Chem. Soc.*, 2007, **129**, 13362; (c) M. Mamada, J. Nishida, D. Kumaki, S. Tokito and Y. Yamashita, *Chem. Mater.*, 2007, **19**, 5404; (d) M.-H. Yoon, S. A. DiBenedetto, M. T. Russell, A. Facchetti and T. J. Marks, *Chem. Mater.*, 2007, **19**, 4864.
- (a) Y. Sakamoto, T. Suzuki, M. Kobayashi, Y. Gao, Y. Fukai, Y. Inoue, F. Sato and S. Tokito, *J. Am. Chem. Soc.*, 2004, **126**, 8138; (b) M. Mushrush, A. Facchetti, M. Lefenfeld, H. E. Katz and T. J. Marks, *J. Am. Chem. Soc.*, 2003, **125**, 9414; (c) M.-H. Yoon, S. A. DiBenedetto, A. Facchetti and T. J. Marks, *J. Am. Chem. Soc.*, 2005, **127**, 1348.
- (a) A. Facchetti, M. Mushrush, H. E. Katz and T. J. Marks, *Adv. Mater.*, 2003, **15**, 33; (b) A. Facchetti, M.-H. Yoon, H. E. Katz, M. Mushrush and T. J. Marks, *Mater. Res. Soc. Symp. Proc.*, 2003, **771**, 397; (c) A. Facchetti, M.-H. Yoon, C. L. Stern, G. R. Hutchison, M. A. Ratner and T. J. Marks, *J. Am. Chem. Soc.*, 2004, **126**, 13480; (d) A. Facchetti, Y. Deng, A. Wang, Y. Koide, H. Sirringhaus, T. J. Marks and R. H. Friend, *Angew. Chem., Int. Ed.*, 2000, **39**, 4547.
- (a) J. A. Letizia, A. Facchetti, C. L. Stern, M. A. Ratner and T. J. Marks, *J. Am. Chem. Soc.*, 2005, **127**, 13476; (b) A. Facchetti, M.-H. Yoon, C. L. Stern, H. E. Katz and T. J. Marks, *Angew. Chem., Int. Ed.*, 2003, **42**, 3900; (c) S. E. Koh, B. Delley, J. E. Medvedeva, A. Facchetti, A. J. Freeman, T. J. Marks and M. A. Ratner, *J. Phys. Chem. B*, 2006, **110**, 24361.
- (a) B. A. Jones, A. Facchetti, T. J. Marks and M. R. Wasielewski, *Chem. Mater.*, 2007, **19**, 2703; (b) X. Cai, M. W. Burand, C. R. Newman, D. A. da Silva Filho, T. M. Pappenfus, M. M. Bader, J.-L. Bredas, K. R. Mann and C. D. Frisbie, *J. Phys. Chem. B*, 2006, **110**, 14590; (c) T. Jung, B. Yoo, L. Wang, B. A. Jones, A. Facchetti, M. R. Wasielewski, T. J. Marks and A. Dodabalapur, *Appl. Phys. Lett.*, 2006, **88**, 183102; (d) B. A. Jones, M. J. Ahrens, M.-H. Yoon, A. Facchetti, T. J. Marks and M. R. Wasielewski, *Angew. Chem., Int. Ed.*, 2004, **43**, 6363–6366; (e) R. J. Chesterfield, C. R. Newman, T. M. Pappenfus, P. C. Ewbank, M. H. Haukaas, K. R. Mann, L. L. Miller and C. D. Frisbie, *Adv. Mater.*, 2003, **15**, 1278; (f) T. M. Pappenfus, R. J. Chesterfield, C. D. Frisbie, K. R. Mann, J. Casado, J. D. Raff and L. L. Miller, *J. Am. Chem. Soc.*, 2002, **124**, 4184.
- S. M. Sze, *Physics of Semiconductor Devices*, 2nd edn, John Wiley & Sons, USA, 1981.
- (a) Y. Li, Y. Wu, P. Liu, Z. Prostran, S. Gardner and B. S. Ong, *Chem. Mater.*, 2007, **19**, 418; (b) M. Akhtaruzzaman, N. Kamata, J. Nishida, S. Ando, H. Tada, M. Tomura and Y. Yamashita, *Chem. Commun.*, 2005, 3183; (c) A. Maliakal, K. Raghavachari, H. E. Katz, E. Chandross and T. Siegrist, *Chem. Mater.*, 2004, **16**, 4980.
- Measured with a Pt working electrode in a dichlorobenzene solution using 0.1 mol dm⁻³ Bu₄NPF₆ as the supporting electrolyte.

- 15 The FET measurements were carried out in vacuum. No change in TFT carrier mobility was observed for p-channel operation of **1–3**-based devices. However electron transport for **DFPADT** was not observed when the devices were tested in air.
- 16 In general, simple SiO₂ hydrocarbon functionalization using octadecyltrichlorosilane (OTS) or hexamethyldisilazane (HMDS) enhances the mobilities and lowers the off-currents of most OTFTs. We reported previously that optimized **DHCO-4T**-based TFTs on HMDS exhibit both p- and n-type transport with carrier mobilities of 0.22 and 0.002 cm² V⁻¹ s⁻¹, respectively. See (a) J. A. Letizia, A. Facchetti, C. L. Stern, M. A. Ratner and T. J. Marks, *J. Am. Chem. Soc.*, 2005, **127**, 13476; (b) M.-H. Yoon, C. Kim, A. Facchetti and T. J. Marks, *J. Am. Chem. Soc.*, 2006, **128**, 12851; (c) I. Yagi, K. Tsukagoshi and W. Aoyagi, *Appl. Phys. Lett.*, 2005, **86**, 103502.
- 17 (a) A. Facchetti, M. Musherush, M.-H. Yoon, G. R. Hutchison, M. A. Ratner and T. J. Marks, *J. Am. Chem. Soc.*, 2004, **126**, 13859; (b) B. A. Jones, M. J. Ahrens, M.-H. Yoon, A. Facchetti, T. J. Marks and M. R. Wasielewski, *Angew. Chem., Int. Ed.*, 2004, **43**, 6363; (c) A. Facchetti, M. Musherush, H. E. Katz and T. J. Marks, *Adv. Mater.*, 2003, **15**, 33; (d) A. Facchetti and T. J. Marks, *Polym. Prepr.*, 2002, **43**(1), 734.
- 18 (a) Y. Kunugi, K. Takimiya, N. Negishi, T. Otsubo and Y. Aso, *J. Mater. Chem.*, 2004, **14**, 2840; (b) T. B. Singh, F. Meghdadi, S. Guenes, N. Marjanovic, G. Horowitz, P. Lang, S. Bauer and N. S. Sariciftci, *Adv. Mater.*, 2005, **17**, 2315; (c) T. Takahashi, T. Takenobu, J. Takeya and Y. Iwasa, *Appl. Phys. Lett.*, 2006, **88**, 033505/1–033505/3.
- 19 The mobility number (0.01 cm² V⁻¹ s⁻¹) slightly lower than the published data (0.02 cm² V⁻¹ s⁻¹) in ref. 6 might be due to the unoptimized deposition conditions in this study.
- 20 M. Yamada, I. Ikemote and H. Kuroda, *Bull. Chem. Soc. Jpn.*, 1988, **61**, 1057.
- 21 However, under similar conditions the electron mobilities for the same TFTs decreased by 30–50%. For example, the mobility had decreased from 1.9 × 10⁻⁴ cm² V⁻¹ s⁻¹ to 5.8 × 10⁻⁵ cm² V⁻¹ s⁻¹ (T_D = 120 °C) and from 2.0 × 10⁻⁴ cm² V⁻¹ s⁻¹ to 1.3 × 10⁻⁴ cm² V⁻¹ s⁻¹ (T_D = 150 °C) on HMDS-treated substrates.
- 22 The *d*-spacing of **ADT (3)** films obtained from XRD is 14.15 Å demonstrating an almost perpendicular orientation of the molecules on the substrate as reported in ref. 6.
- 23 C. Kim, A. Facchetti and T. J. Marks, *Science*, 2007, **318**, 76.